Accepted Manuscript

Conversion of a digital camera into a non-contact colorimeter for use in stone cultural heritage: the application case to Spanish granites

Patricia Sanmartín, Elisabet Chorro, Daniel Vázquez-Nion, Francisco Miguel Martínez-Verdú, Beatriz Prieto

PII: S0263-2241(14)00284-X
DOI: http://dx.doi.org/10.1016/j.measurement.2014.06.023
Reference: MEASUR 2910

To appear in: *Measurement*

Received Date: 26 March 2014
Revised Date: 28 May 2014
Accepted Date: 23 June 2014

Please cite this article as: P. Sanmartín, E. Chorro, D. Vázquez-Nion, F.M. Martínez-Verdú, B. Prieto, Conversion of a digital camera into a non-contact colorimeter for use in stone cultural heritage: the application case to Spanish granites, *Measurement* (2014), doi: http://dx.doi.org/10.1016/j.measurement.2014.06.023

This is a PDF file of an unedited manuscript that has been accepted for publication. As a service to our customers we are providing this early version of the manuscript. The manuscript will undergo copyediting, typesetting, and review of the resulting proof before it is published in its final form. Please note that during the production process errors may be discovered which could affect the content, and all legal disclaimers that apply to the journal pertain.

ACCEPTED MANUSCRIPT

Conversion of a digital camera into a non-contact colorimeter for use in stone cultural heritage: the application case to Spanish granites

Patricia Sanmartín[1*], Elisabet Chorro[2], Daniel Vázquez-Nion[1], Francisco Miguel Martínez-Verdú[2], Beatriz Prieto[1]

1. Departamento de Edafología y Química Agrícola. Facultad Farmacia. Universidad de Santiago de Compostela, 15782 - Santiago de Compostela, Spain.
2. Color & Vision Group, University Institute of Physics Applied to Sciences and Technologies. University of Alicante, San Vicente del Raspeig, 03690-Alicante, Spain.

*Corresponding author: Patricia Sanmartín
Departamento de Edafología y Química Agrícola
Facultad de Farmacia. Campus Vida
Universidad de Santiago de Compostela
15782 Santiago de Compostela. SPAIN
Telephone: +34 881 814920 Fax: +34 881 815106
E-mail address: patricia.sanmartin@usc.es
http://www.usc.es

Current address:
Prof. Ralph Mitchell's Laboratory of Applied Microbiology
Engineering Science Building, 58 Oxford St. Cambridge, MA 02138. USA
Harvard School of Engineering and Applied Sciences (SEAS)
HARVARD

ACCEPTED MANUSCRIPT

ACCEPTED MANUSCRIPT

Abstract

In this study, a digital CMOS camera was calibrated for use as a non-contact colorimeter for measuring the color of granite artworks. The low chroma values of the granite, which yield similar stimulation of the three color channels of the camera, proved to be the most challenging aspect of the task. The appropriate parameters for converting the device-dependent RGB color space into a device-independent color space were established. For this purpose, the color of a large number of Munsell samples (corresponding to the previously defined color gamut of granite) was measured with a digital camera and with a spectrophotomer (reference instrument). The color data were then compared using the CIELAB color formulae. The best correlations between measurements were obtained when the camera works to 10-bits and the spectrophotometric measures in SCI mode. Finally, the calibrated instrument was used successfully to measure the color of six commercial varieties of Spanish granite.

Keywords**:** CIELAB system; CMOS camera; color calibration; cultural heritage; granite; ornamental stone; RGB values.

ACCEPTED MANUSCRIPT

ACCEPTED MANUSCRIPT

1. Introduction

Color is one of the most important visual properties of ornamental and monumental stone. Color changes caused by weathering and decay greatly influence the aesthetic value of stone. Extent of such change can be quantified by contact-type color measuring devices (colorimeters and spectrophotometers [1-6]) and analyzed in a device-independent color space, such as CIE-XYZ or CIE-L*a*b*. But these devices present some limitations: (1) sometimes is not possible to reach the target object with the instrument, (2) they are more expensive and complex than other non-dedicated color measuring devices (digital cameras, scanners and even mobile-phone cameras) and (3) as the field of view of contact-type color devices is limited, measurement of heterogeneous surfaces produces unrealistic color values. To overcome these limitations, digital cameras can be used because (1) the field of view is only limited by the size of the appropriately illuminated area, (2) contact with the target object is not required, and (3) they encode each point of the entire surface simultaneously, thus quantifying surface characteristics and defects.

Digital cameras only detect changes in light intensity, not color. To encode color, they require three different filters in addition to the sensors. These filters usually have spectral bands in the red (R), green (G) and blue (B) regions, and therefore the encoded values are RGB digital values. RGB is a device-dependent color space as the filters and other parameters are specific to individual cameras and can be changed with camera settings such as the spectral exposure level, white balance and the dynamic range. As RGB values cannot be transformed to XYZ or L*a*b* values directly by using a standard formula, a transformation that defines the mapping between RGB digital values and a device independent color space is necessary. This process is known as camera characterization [7]. Several camera characterization techniques have been used with the aim of developing a model (and estimating its parameters) for obtaining L*a*b* color measurements from RGB digital values (e.g. [7-15]). In general, these techniques can be divided into two categories: (1) *spectral characterization*, which measures the three spectral-sensitivity functions for the red-green-blue (RGB) channels and requires a monochromator and a radiance meter [16]; and (2) *colorimetric characterization*, which involves mathematical transformations that yield the tristimulus values from the digital values and which require use of a reference target that contains a certain number of color samples. In the present study, we used the latter color target-based approach, which only requires a certain number of color samples and is, therefore, a more practical method [7]. We chose target-based characterization procedure described by Hong et al. [7], which is based on polynomial modeling. This calibration model has been used successfully in nearly two hundred scientific papers with different objectives, e.g., to determine how facial skin coloration affects perceived health of human faces [17, 18] and for use in dental color matching [19].

ACCEPTED MANUSCRIPT

In the field of lithology, the image captured by the camera is usually processed by different segmentation strategies. For example, one innovative application focuses on the segmentation of decay zones from images of stone materials [20, 21]. Another strategy enables improvement and semi-automatization of the study of chemical decay causing visible changes in color of some regions [22]. A portable stereo active vision system (AVS) has also been specifically designed to perform on-site processing of the data acquired in the field of cultural heritage conservation [23]. Moreover, the digital decorrelation of RGB images by Principal Components Analysis (PCA) enables contrast enhancement of minority elements apparently absent from the initial RGB digital image [24-27]. Camera characterization has been used in very few studies, including that of Chorro et al. [28], who used the sRGB model to predict the CIE-XYZ tristimulus values depending on the RGB digital data, with the final aim of quantifying color changes in the appearance of a paving stone (marble) in relation to the viewing distance. More recently, Concha-Lozano et al. [29] used spectroradiometric measurements to calibrate a camera in order to establish the color ranges within which replacement of biodetritic limestone in medieval walls will be imperceptible. Nevertheless, to our knowledge, camera characterization has not previously been reported for granite. Measurement of the color of granite is complicated by the low chroma and spatially heterogeneous color, which is formed by the different colors of the constituent minerals. There is great interest in measuring the color of granite because, amongst other reasons, granite is one of the most commonly used types of igneous rock owing to its abundance and great variety of color and textures, and because it is a major construction material in European historical buildings and monuments [30].

The present study focused on developing a method of RGB digital camera colorimetric characterization for studying stone, specifically granite. The nearly neutral colors of granite yield similar stimulation of the three color channels of the camera (red, green and blue), which makes the task in hand particularly challenging. For the first time, the settings of a digital camera have been adjusted to obtain the camera response closest to that of the reference instrument (spectrophotometer) for granite color measurement using the CIELAB system. The developed method was successfully used to measure the color of granite samples. This is of particular interest in the field of stone conservation, in which innovative non-invasive tools for monitoring the aesthetic changes in stone surfaces are required.

2. Experimental

2.1. Fine-tuning of the camera calibration method

The methodology developed for estimating the RGB→L*a*b* transformation consisted of two parts. In the first part, we determined the appropriate settings and working conditions of the acquisition system (camera) and reference instrument (spectrophotometer). In the second part, we selected a large set of Munsell matte and glossy samples corresponding to the previously defined color gamut of granite [31]. The colors of these samples were measured using both devices under the conditions

ACCEPTED MANUSCRIPT

ACCEPTED MANUSCRIPT

indicated in the first part. The digital images were obtained with the following image acquisition system (*Figure 1*):

- PixeLINK PL-A782 color digital camera, 2008 (suitable for industrial use), with CMOS sensor architecture, 6.6 Mega Pixels of resolution and a user-selectable 8 or 10-bit output. The camera was placed vertically at a distance of 112 cm from the sample. The angle between the axis of the camera and the source of illumination was approximately 45º. Thus, following the CIE nomenclature [32], the measurement geometry was 45ºx90º or 45/0, which is very common in industrial applications in order to avoid specular reflection.
- Camera lens: Fujinon CF50HA-1, 50 mm focal length, 1", designed to be used with high resolution cameras with images up to 1.5 Megapixels, with manual iris and focus.
- Lighting was achieved with Kaiser RB-5004-HF high frequency daylight copy light set with four Oxram Dulux L 36W/954 fluorescent light tubes (41.5 cm in length), with a correlated color temperature of 5400 K (natural daylight) and a color rendering index (R_a) close to 90%.
- The room where images were taken was totally dark and a black cloth was placed on the floor under the table used as the sample stand, to minimize background light.
- The size of the captured images was 240 pixels (width) by 192 pixels (height). The pixel size was 347 x 375 μm^2. The images were stored in uncompressed tagged image format files (TIFF).
- The camera settings used in the present study are summarized in *Figure 2*. The main purpose of this step was to maintain constant any software camera control (white balance, exposure time, gain, etc) to obtain a stable, reliable and reproducible RGB color space, although this would presumably limit the dynamic range of luminance of the camera [33].

The lighting level, and its uniformity, is critical for image acquisition, so that the camera can deliver meaningful, repeatable data [34]. Therefore, the lighting map for the reference target needs to be as spatially and temporally uniform as possible. The uniformity of light intensity was tested using a radiometer (DHD 2302.0, HERTER) (*Figure 3*).

However, the combination of lens aperture size and exposure time determines the amount of light reaching the CMOS sensor of the camera. Obviously, the signals generated by the CMOS sensor vary with the amount of light reaching CMOS sensor. Therefore, both aperture size (*f*/4) and exposure time (99.537 ms, milliseconds) were fixed during the period of image acquisition. We also totally occluded the camera-lens aperture for the black reference, and we captured a standard white reference plate for the white reference.

ACCEPTED MANUSCRIPT

The camera is capable of both 8-bit depth and 10-bit depth linear data acquisition; both were used in the present study. 8-bit data can hold $2^8 = 256$ possible values ranging from 0 to 255. For an RGB image in which the values are 8-bit unsigned integers, 0 0 0 represents black, 255 255 255 represents white, 255 0 0 represent red, 0 255 0 represents green, and 0 0 255 represents blue. 10-bit data yields $2^{10} = 1024$ possible values, ranging from 0 to 1023. For an RGB image in which the values are 10-bit unsigned integers, 0 0 0 represents black, 1023 1023 1023 represents white, 1023 0 0 represents red, 0 1023 0 represents green, and 0 0 1023 represents blue. Special attention was paid to setting the exposure to avoid any “color clipping” for the white reference, i.e., saturation of one or more of the three RGB channels, obtaining R, G or B values above 255 with 8-bit data and 1023 with 10-bit data [7, 13].

The spectrophotometer used was a portable spectrophotometer (Konica Minolta CM-700d) equipped with CM-S100w (SpectraMagicTM NX) software. The measuring conditions were illuminant D65, observer 2º and a 3-mm diameter viewing area. Measurements were made in both specular component included (SCI) and specular component excluded (SCE) modes to determine which mode approximates better to the camera vision. The SCI mode, in which the gloss trap of the spectrophotometer is closed, includes the total reflectance (considering both specular and diffuse reflections); the SCE mode, in which the gloss trap is open, includes the diffuse reflectance and excludes most of the specular component and is therefore more sensitive to color differences due to differences in surface roughness [31, 35]. It is generally accepted in the field of color science that the SCE mode approximates the view with the naked eye and the SCI mode is adequate for analyzing the intrinsic color of objects [31, 36].

In attempting to adjust the camera settings to make the camera response more similar to the reference-instrument response in the CIELAB system, standard color targets consisting of an assortment of color patches are commonly applied. The Gretag Macbeth color-checker color rendition chart [37] is one of the most commonly used, although it consists of only 24 patches. In some cases, as in the second part of our camera characterization method, a customized characterization target, consisting of a large number of patches, was designed and applied. Thus, a set of samples (212 Munsell color charts, 125 from the glossy and 87 from the matte collection), corresponding to the three-dimensional color area of the CIELAB space, in which the color of the ornamental granites is defined [31] was selected. In each of the 212 color samples, the L*a*b* color values were measured using the portable spectrophotometer under the measuring conditions described above. One reading was taken per sample. An RGB digital image was also taken of each Munsell sample/chip. The digital camera was placed orthogonally to the Munsell sample. The field of view of the camera was fully occupied by a single Munsell chip. Thus, 212 RGB measurements, i.e., R, G and B color values, were obtained. Note that the granite color is located in the nearly neutral region of CIELAB color space, far from the highly saturated colors like intense or pure yellows, reds and greens. This makes it difficult for the instrument to measure the color, as the nearly neutral colors yield similar stimulation of the three color channels (red,

ACCEPTED MANUSCRIPT

ACCEPTED MANUSCRIPT

green, and blue) of the camera, and the differences between these colors constitute small variations in a high nearly constant background signal [10].

2.2. Performance testing and verification of the resulting calibration

To confirm selection of the camera working conditions, the method described in Section 2.1 was applied to the color characterization of granite samples. Six commercial varieties of granite (*Aldán*, *Blanco Cristal*, *Grissal*, *Monte Enxa*, *Rosa Porriño* and *Silvestre*) were considered. Data on the origin, geochemistry and textural and mineral characteristics of each type of granite are shown in **Table 1.** Five square specimens (25 or 36cm^2) of each type of granite were prepared with a honed surface finish. An image of each specimen was taken using the image acquisition system described in Section 2.1. During the process, each of the samples was placed on the marked area of a light table. The measurement area in the specimens was approximately 6.25 cm^2 (width, 25 mm and length, 25 mm). The color of granite samples was then measured with a portable spectrophotometer (Konica Minolta CM-700d) equipped with CM-S100w (SpectraMagicTM NX) software, following the working methodology designed by Prieto et al. [38]. The measuring conditions and specular component modes were the same as those used to measure the Munsell samples (see Section 2.1).

3. Results and discussion

The stability of the light source was evaluated prior to establishing the color measurement protocol for the study. Figure 3 shows the light levels (in millilux = 10^{-3} lux or lx) across the table top. The light was not completely homogeneous and varied from 1560 ± 20 lx at the upper center to 2400 ± 20 lx to the right and left of the middle-center. An area of the table where the percentage of light level (in millilux) did not vary by more than 3% was marked. The average level of lighting was 1780 ± 20 lx within this area, which is where the images were captured.

The color of the 212 test samples (Section 2.1) was measured using both devices. Hong et al. [7] noted that better results can be achieved if more terms (e.g. R^2, G^2, B^2, etc) are included to the matrix derived by the characterization process of the digital camera. In the present study, a third order polynomial (matrix with 20 terms) was used. This can be expressed as follows [9]:

$$D = \begin{bmatrix} L_1^* & a_1^* & b_1^* \\ \vdots & \vdots & \vdots \\ L_n^* & a_n^* & b_n^* \end{bmatrix} \quad (1)$$

$$V = \begin{bmatrix} 1 & R_1 & G_1 & B_1 & R_1G_1 & R_1B_1 & \cdots & R_1^3 & G_1^3 & B_1^3 \\ \vdots & \vdots & \vdots & \vdots & \vdots & \vdots & \cdots & \vdots & \vdots & \vdots \\ 1 & R_n & G_n & B_n & R_nG_n & R_nB_n & \cdots & R_n^3 & G_n^3 & B_n^3 \end{bmatrix} \quad (2)$$

ACCEPTED MANUSCRIPT

$$D = M \cdot V \tag{3}$$

$$M = \left[m_{ij}\right]_{3x20} = \left[(V^t \cdot V)^{-1} V^t \cdot D\right]^t \tag{4}$$

where M is the matrix with the transformation polynomial coefficients characterizing the camera, $\{R_n, G_n, B_n\}$ are the digital levels of the training color patches (i.e. 212 color charts-Section 2.1) measured by the camera and $\{L^*_n, a^*_n, b^*_n\}$ are the CIE-L*a*b* values of the training set (i.e. 212 color charts-Section 2.1) measured by the spectrophotometer. Finally, transformation of the RGB values was achieved by using the following equation:

$$\begin{bmatrix} L^* \\ a^* \\ b^* \end{bmatrix} = \left[m_{ij}\right]_{3x20} \cdot \begin{bmatrix} 1 \\ R \\ G \\ B \\ RG \\ \vdots \\ B^3 \end{bmatrix}_{20x1} \tag{5}$$

The absolute color measurement by the camera, calculated using Eq. (5), in both 8 and 10-bits of color depth, was compared with the external reference provided by the spectrophotometer, in both specular component included (SCI) and excluded (SCE) modes. The CIELAB coordinates of each measured chip, obtained separately by the camera and the reference instrument were compared, taking into account the classical CIELAB formula (ΔE^*_{ab}) and the other color difference formulae based on CIELAB space (ΔE_{94}, ΔE_{00} and CMC). The results obtained are shown in **Table 2**, which includes the average, maximal and minimal values of the computed total color differences, *viz.* ΔE^*_{ab}, ΔE_{94} (2:1:1), ΔE_{94} (1:1:1), ΔE_{00} (2:1:1), ΔE_{00} (1:1:1), CMC (2:1) and CMC (1:1). No equivalence of scale factor was found in the values calculated using the different formulae considered, as reported by Prieto et al. [38] on comparing the results obtained by measuring granite samples with the different reading areas (or measuring head sizes) of a spectrophotometer and a colorimeter. It is difficult to specify admissible color differences between devices, because most recommendations on color differences refer to situations in which the colors of different objects are measured under the same illuminant, unlike in the present study (Section 2.1). The color-tolerance concept is based on color discrimination, which largely depends on observational conditions. In this case, we should take into account that the color of the sample was viewed with different illumination, leading to greater color tolerance. For instance, analysis of the color differences in both natural and artificial objects over one day revealed values exceeding 3 CIELAB units when the color of the objects under the maximum solar elevation was compared with that at twilight [39]. Based on these findings, consideration of 1 CIELAB unit as the visual color difference threshold or just noticeable difference (jnd), which constitutes the lower limit of perception in an individual with normal color vision [35, 40] appears too strict in this case. Likewise 1.75 CIELAB units, considered as the suprathreshold color-difference [41]. Thus, we decided to consider for evaluation of the results perceptual limits starting from 3 CIELAB units and taking into account the following established thresholds: (1) the normal color tolerance, specified by Lozano [42] as being between 2.8 and 5.6 CIELAB

ACCEPTED MANUSCRIPT

ACCEPTED MANUSCRIPT

units (according to the usual conversion factors between color-difference units [40]); (2) the acceptable color tolerance of 3 CIELAB units [43, 44]; (3) the normal limit of perception in industrial or technical applications of 5 CIELAB units [45-47], and (4) the perceptible but acceptable difference in color of 6 CIELAB units considered by Hardeberg [48]. We found that the average total color differences obtained, ranging from 1.9 to 1.1 CIELAB units (**Table 2**), are nearly undetectable to the untrained eye. The maximal total color differences, with values ranging from 3.7 to 6.9 CIELAB units, must be considered virtually acceptable for most industrial applications. Furthermore, the color difference formulae based on CIELAB space include three parametric factors, k_L, k_C and k_H, which are correction terms for the variation in experimental conditions. Under reference conditions, these are all set at 1 [32]. However, in the present study, the illumination conditions were not reference conditions and the samples were not homogeneously colored. For textured samples, it is not clear which values should be used for the parametric factors [49-51]. Considering an increase in the relative contribution of the lightness term (k_L parametric factor 2, instead of 1) in the color difference formulae, the maximum value decreased greatly by between 2 and 3 CIELAB units, and only reached values of between 3.7 and 3.9 CIELAB units (**Table 2**). So, depending on the used color difference formula, the better setting could be different. However, as it can be observed in the **Table 2**, if we adopt the maximal value of the total color differences as the criterion of choice, in all cases except ΔE00 (2:1:1), these differences are lesser when the spectrophotometer on specular component included (SCI) mode and the digital camera with 10-bits data acquisition were used. Likewise, although with other combinations, the average total color differences were slightly lower (maximum 0.4 CIELAB units lower with respect the conditions just cited), in those cases were also achieved the biggest maximal color differences (up to 9.5 CIELAB units of difference with respect to the above cited conditions). Consequently and considering the lowest maximal value of the total color differences as the selection criterion, although also comparing its results with the average and maximum values of total color differences, the digital camera 10-bit depth linear data acquisition is the best for our purpose and should be compared with SCI spectrophotometric data.

In the cultural heritage field, most colorimetric measurements are used to estimate color differences (e.g. [6, 52]). Therefore, to calibrate a digital camera as a colorimeter for use in this field, it is advisable to explore the discriminatory capacity of the camera and its reliability for measuring small differences between very similar colors. A certain number of color differences between pairs of nearest-neighbor chips were calculated separately by both the camera and the reference instrument, according to the classical CIELAB formula (ΔE^*_{ab}) and other color difference formulae based on the CIELAB space (ΔE_{94}, ΔE_{00} and CMC). Comparison of the results obtained with the camera and the reference instrument indicated the discrepancy between the two devices. This discrepancy was used to test the reliability of the camera performance and was compared with the precision and tolerance of the devices (**Tables 3 and 4**). More than half of the absolute discrepancies exceed the suprathreshold value for visual discrimination of 0.887 CIELAB units [41]. Nonetheless, the values of the relative discrepancy were very low and although the absolute discrepancy exceeded the uncertainty or precision of both devices, it remained within the camera tolerance (1.32 ± 1.06 vs. 2.4 CIELAB units). Thus, the camera and reference instrument showed a high

ACCEPTED MANUSCRIPT

degree of consistency in the estimation of small color differences, and therefore the camera performed well [53].

The selected camera working conditions were then used to characterize the color of six commercial varieties of granite (*Aldán*, *Blanco Cristal*, *Grissal*, *Monte Enxa*, *Rosa Porriño* and *Silvestre*). The results obtained (*Figure 4*) appeared sufficiently accurate and reliable: considering the set of samples, regardless of type of granite and granite sample, the total color difference (ΔE^*_{ab}) between the measured granite color (using the spectrophotometer in specular component included (SCI) mode) and the estimated granite color (using the digital camera with 10-bits data acquisition) was generally below 6 CIELAB units. Specifically, the ΔE^*_{ab} values ranged between 2.7 and 5.5 CIELAB units for *Grissal* and 3.4 and 5.1 CIELAB units for *Blanco Cristal,* indicating that, with the measurement method used, the best results were obtained with achromatic rocks. The values of ΔE^*_{ab} for *Monte Enxa* and *Rosa Porriño* ranged from 4.4 to 6.6 and from 4.3 to 7.0, respectively. These were the largest color differences reached in the study and corresponded to those types of granite in which the color is farthest from the achromatic area. Intermediate values of ΔE^*_{ab} were obtained for *Aldán*, with values within the range of 3.0 - 6.5 CIELAB units, and for *Silvestre*, with values within the range 3.3 - 5.5 CIELAB units. In this case, differences of 6 CIELAB units cannot be considered high as two different devices with different lighting conditions were used. For granite color measurements, differences of nearly 3 CIELAB units are obtained, even when using the same device with different measuring heads [38]. Moreover, the limits of perception are usually calculated for homogeneous samples (in terms of color and texture) (for further details, see, e.g. [54]), unlike the granite samples that were the target of the present study.

4. Conclusions

A calibration procedure was developed for granite color measurement using a non-contact device (a CMOS digital camera). Working conditions for the reference instrument (spectrophotometer) and the digital camera were examined to ensure the best possible correlation between both devices. An improvement was obtained by quantizing the camera RGB values to 10-bits relative to those recorded in 8-bits. Likewise, better results were achieved with the specular component included (SCI) mode than with the specular component excluded (SCE) mode in the reference instrument (spectrophotometer).

The resulting calibration was successfully applied to six commercial varieties of granite, and the differences between data obtained with the reference instrument and with the camera calibrated as colorimeter were no higher than 6 CIELAB units.

This method, which enables RGB data to be expressed as device independent L*a*b* data, without introducing a noticeable amount of error, is sufficiently adaptable to be transposed to any computer vision system that can produce consistent RGB source data. The method can be used in many industrial applications using textured colored

ACCEPTED MANUSCRIPT

materials and products. Apart from the fact that contact is not required for the color measurement, the other main advantage is the flexibility afforded by the choice of the size of the area to be characterized, which can range from small areas (347 x 375 pixel size μm2) to areas as large as allowed by the lens size.

Acknowledgements

The present study was financially supported by the Xunta de Galicia (09TMT014203PR) and the European Union and Spanish Ministry of Economy and Competitiveness under grants DPI2008-06455-C02-02 and DPI2011-30090-C02-02. Dr. Patricia Sanmartín acknowledges a scholarship for postgraduate studies abroad (2012 Call) from Barrié de la Maza Foundation. She is currently supported by a postdoctoral contract within the framework of the 2011-2015 Galician Plan for Research, Innovation and Growth (Plan I2C) for the year 2012.

References

[1] D.L. MacAdam, Colour Measurement –Theme and Variations, Second Revised Edition, Springer-Verlag, 1985.

[2] H.A.Viles, M.P. Taylor, T.J.S. Yates, S.W. Massey, Soiling and decay of NMEP limestone tablets, Sci Total Environ 292 (2002) 215–229.

[3] H.A. Viles, A.A. Gorbushina, Soiling and microbial colonization on urban roadside limestone: a three year study in Oxford, England, Build Environ 38 (2003) 1217–1224.

[4] M. Thornbush, H.A. Viles, Changing patterns of soiling and microbial growth on building stone in Oxford, England after implementation of a major traffic scheme, Sci Total Environ 367 (2006) 203–211.

[5] C.M. Grossi, P. Brimblecombe, R.M. Esbert, F.J. Alonso, Color changes in architectural limestones from pollution and cleaning, Color Res Appl 32 (2007) 320–331.

[6] P. Sanmartín, D. Vázquez-Nion, B. Silva, B. Prieto, Spectrophotometric color measurement for early detection and monitoring of greening on granite buildings, Biofouling 28(3) (2012) 329–338.

[7] G. Hong, M.R. Luo, P.A. Rhodes, A study of digital camera colorimetric characterization based on polynomial modeling, Color Res Appl 26(1) (2001) 76–84.

[8] R. Blasubramanian, Device characterization. In: Sharma, G. (ed.), Digital Color Imaging Handbook, Boca Raton: CRC Press, chap. 5, 2003.

ACCEPTED MANUSCRIPT

ACCEPTED MANUSCRIPT

[9] F. Martínez-Verdú, E. Chorro, E. Perales, M. Vilaseca, J. Pujol, Camera based colour measurement. In: Gulrajani, M.J. (ed.), Colour measurements: principles, advances and industrial applications, New Delhi: Woodhead Publishing, chap. 6, 2010.

[10] M.S. Millán, E. Valencia, M. Corbalán, 3CCD Camera's capability for measuring color differences: experiment in the nearly neutral region, App Opt 43(36) (2004) 6523-6535.

[11] P.L. Vora, J.E. Farrell, J.D. Tietz, D.H. Brainard, Digital color cameras. 1. Response models. Tech Rep HPL-97-53. Hewlett-Packard Laboratory, Palo Alto, California, http:www.hpl.hp.com_techreports_97_HPL-97-53.html, 1997.

[12] P. Laflaquiere, D. Lafon, O. Eterradossi, P. Slangen, Characterization of color texture: CIEL*a*b* calibration of CCD device. Proc SPIE 3409, 118–128, 1998.

[13] F. Martínez-Verdú, J. Pujol, P. Capilla, Characterization of a digital camera as an absolute tristimulus colorimeter, J Imaging Sci Technol 47 (2003) 279–295.

[14] K. Leon, D. Mery, F. Pedreschi, J. Leon, Color measurement in L*a*b* units from RGB digital images, Food Res Int 39 (2006) 1084–1091.

[15] R.E. Larraín, D.M. Schaefer, J.D. Reed, Use of digital images to estimate CIE color coordinates of beef, Food Res Int 41(4) (2008) 380–385.

[16] R.S. Berns, M.J. Shyu, Colorimetric characterization of a desktop drum scanner using a spectral model, J Electron Imaging 4 (1995) 360-372.

[17] I.D. Stephen, M.J.L. Smith, M.R. Stirrat, D.I. Perrett, Facial Skin Coloration Affects Perceived Health of Human Faces, Int J Primatol 30(6) (2009) 845-857.

[18] I.D. Stephen, V. Coetzee, D.I. Perrett, Carotenoid and melanin pigment coloration affect perceived human health, Evol Hum Behav 32(3) (2011) 216-227.

[19] L. Gómez-Robledo, N. López-Ruiz, M. Melgosa, A.J. Palma, L.F. Capitán-Vallvey, M. Sánchez-Marañón, Using the mobile phone as Munsell soil-colour sensor: An experiment under controlled illumination conditions, Comput Electron Agr 99 (2013) 200–208.

[20] R. Cossu, L. Chiappini, A color image segmentation method as used in the study of ancient monument decay, J Cult Heritage 5 (2004) 385–391.

[21] M.M. Cerimele, R. Cossu, Decay regions segmentation from color images of ancient monuments using fast marching method, J Cult Heritage 8 (2007) 170–175.

ACCEPTED MANUSCRIPT

ACCEPTED MANUSCRIPT

[22] L. Appolonia, V. Bruni, R. Cossu, D. Vitulano, Computer-aided monitoring of buildings of historical importance based on color, J Cult Heritage 7 (2006) 85–91.

[23] A. Balsamo, A. Chimienti, P. Grattoni, R. Nerino, G. Pettiti, M.L. Rastello, M. Spertino, Active vision applications to cultural heritage acquisition and monitoring, J Cult Heritage 7 (2006) 98–109.

[24] A.Z. Miller, N. Leal, L. Laiz, M.A. Rogerio-Candelera, R.J.C. Silva, A. Dionisio, M.F. Macedo, C. Saiz-Jimenez, Primary bioreceptivity of limestones used in Southern Europe monuments. In: Smith, B.J., Gomez-Heras, M., Viles, H.A., Cassar, J. (eds.), Limestone in the Built Environment: Present Day Challenges for the Preservation of the Past. J Geol Soc, Special Publications 331 (2010) 79-92.

[25] A.Z. Miller, M.A. Rogerio-Candelera, L. Laiz, J. Wierzchos, C. Ascaso, M.A. Sequeira Braga, M. Hernández-Mariné, A. Maurício, A. Dionísio, M.F. Macedo, C. Saiz-Jimenez, Laboratory-induced endolithic growth in calcarenites: biodeteriorating potential assessment, Microbial Ecol 60 (2010) 55-68.

[26] A.Z. Miller, M.A. Rogerio-Candelera, A. Dionísio, M.F. Macedo, C. Saiz-Jimenez, Microalgae as biodeteriogens of stone cultural heritage: qualitative and quantitative research by non-contact techniques. In: Columbus, F. (ed.), Microalgae: Biotechnology, Microbiology and Energy. Nova Science Publishers, pp.345-358, 2011.

[27] M.A. Rogerio-Candelera, Una propuesta no invasiva para la documentacion integral del arte rupestre (In Spanish). PhD thesis, Universidad de Sevilla, Spain, 2008.

[28] E. Chorro, E. Perales, D. de Fez, M.J. Luque, F.M. Martinez-Verdu, Application of the S-CIELAB color model to processed and calbrated images with a colorimetric dithering method, Opt Express 15 (2007) 7810–7817.

[29] N. Concha-Lozano, D. Lafon, N. Sabiri, P. Gaudon, Color Thresholds for Aesthetically Compatible Replacement of Stones on Monuments, Color Res Appl 38(5) (2013) 356-363.

[30] M.A. Vicente, J. Delgado Rodrigues, J. Acevedo, Degradation and Conservation of Granitic Rocks in Monument. Protection and Conservation of the European Cultural Heritage Research Report No. 5, European Commission: Brussels, Belgium, 1996.

[31] P. Sanmartín, B. Silva, B. Prieto, Effect of surface finish on roughness, color and gloss of ornamental granites, J Mater Civil Eng 23(8) (2011) 1239–1248.

[32] CIE Publication 15:2004. Commission Internationale de l'Eclairage, Vienna, 2004.

ACCEPTED MANUSCRIPT

[33] M. de Lasarte, M. Arjona, M. Vilaseca, F.M. Martínez-Verdú, J. Pujol, Luminance adaptation model for increasing the dynamic range of an imaging system based on a CCD camera, Optik 122(15) (2011) 1367-1372.

[34] R.W.G. Hunt, Measuring colour, second edition. (Ellis Horwood series in applied science and industrial technology). Ellis Horwood Limited, 1995.

[35] G. Wyszecki, W.S. Stiles, Color Science. Concepts and Methods, Quantitative Data and Formulae. John Wiley and Sons: New York, 1982.

[36] Y. Hosoya, T. Shiraishi, T. Odatsu, T. Ogata, M. Miyazaki, J.M. Powers, Effects of specular component and polishing on color of resin composites, J Oral Sci 52(4) (2010) 599-607.

[37] C.S. McCamy, H. Marcus, J.G. Davidson, A Color-Rendition Chart, J Appl Photogr Eng 2(3) (1976) 95–99.

[38] B. Prieto, P. Sanmartín, B. Silva, F. Martinez-Verdú, Measuring the color of granite rocks: A proposed procedure, Color Res Appl 35(5) (2010) 368-375.

[39] J. Romero, J. Hernández-Andrés, J.L. Nieves, J.A. García, Color coordinates of objects with daylight changes, Color Res Appl 28 (2003) 25–35.

[40] M. Melgosa, J.J. Quesada, E. Hita, Uniformity of some recent color metrics tested with an accurate color-difference tolerance dataset, Appl Optics 33(34) (1994) 8069-8077.

[41] M. Melgosa, E. Hita, A.J. Poza, D.H. Alman, R.S. Berns, Suprathreshold color-difference ellipsoids for surface colors, Color Res Appl 22 (1997) 148–155.

[42] R.D. Lozano, El color y su medición. AmericaLee: Buenos Aires, 1978.

[43] R.S. Berns, Billmeyer and Saltzman´s Principles of Color Technology, 3rd Ed. John Wiley and Sons: New York, 2000.

[44] H.G. Völz, Industrial color testing. Wiley –VCH: Weinheim, 2001.

[45] S. Palazzi, Colorimetria, La scienza del colore nell’arte e nella técnica. Nardini Editore: Florence, Italy, 1995.

[46] J.L. Nieves, F. Pérez-Ocón, J. Hernández-Andrés, J. Romero, Spectral-reflectance function recovery for improved colour-constancy experiments, Displays 23(5) (2002) 213–222.

ACCEPTED MANUSCRIPT

ACCEPTED MANUSCRIPT

[47] F. Cappitelli, E. Zanardini, G. Ranalli, E. Mello, D. Daffonchio, C. Sorlini, Improved methodology for bioremoval of black crusts on historical stone artworks by use of sulfate-reducing bacteria, Appl Environ Microb 72 (2006) 3733-3737.

[48] J.Y. Hardeberg, Acquisition and reproduction of color images: colorimetric and multispectral approaches. PhD Thesis, Ecole Nationale Superieure des Telecommunications, Paris, 1999.

[49] CIE Publication 101:1993. Parametric effects in colour-difference evaluation. Central Bureau of CIE, Vienna, 1993.

[50] M. Lucassen, P. Bijl, The CIE94 colour difference formula for describing visual detection thresholds in static noise. In: CGIV 2004 - Second European Conference on Color in Graphics, Imaging, and Vision and Sixth International Symposium on Multispectral Color Science, 2004.

[51] H. Liu, M. Huang, G. Cui, M.R. Luo, M. Melgosa, Color-difference evaluation for digital images using a categorical judgment method, J Opt Soc Am A Opt Image Sci Vis 30(4) (2013) 616-626.

[52] B. Prieto, B. Silva, N. Aira, L. Laiz, Induction of biofilms on quartz surfaces as a means of reducing the visual impact of quartz quarries, Biofouling 21 (2005) 237–246.

[53] E. Valencia Díaz, Procesado de imagen digital en color: Adquisición, Análisis Colorimétrico y Realce (In Spanish). PhD Thesis, Universitat Politècnica de Catalunya, Spain, 2007.

[54] J. Schanda, Colorimetry: Understanding the CIE system. John Wiley & Sons: New York, 2007.

[55] P. Sanmartín, Evaluación de dos tratamientos consolidantes aplicados a granitos y calcarenitas (In Spanish). Supervised research project, Universidade de Santiago de Compostela, Spain, 2007.

[56] B. Prieto, B. Silva, Estimation of the potential bioreceptivity of granitic rocks from their intrinsic properties, Int Biodeter Biodegr 56 (2005) 206–215.

Capture figures:

Figure 1. Image acquisition system setup. (a) Laboratory computer vision and capture system, (b) PL-A782 CMOS digital camera.

ACCEPTED MANUSCRIPT

ACCEPTED MANUSCRIPT

Figure 2. Screenshot of the camera settings conditions, showing the exposure time, saturation, white balance and image format file (TIFF).

Figure 3. Camera-light configuration. (a) Light sources aligned 45º with the camera's optical axis. Control for lighting or illuminance level was performed with a radiometer. (b) Results achieved with the radiometer (in millilux, 10^{-3} lx) appear across the table. White numbers indicate the area where the percentage of light level did not vary by more than 3% and because of that, the images were taken inside that area.

Figure 4. Total color difference (ΔE^*_{ab}) between data obtained with spectrophotometer and camera for the six commercial varieties of granite. Five specimens (represented by different bars) were measured for each variety of granite.

ACCEPTED MANUSCRIPT

ACCEPTED MANUSCRIPT

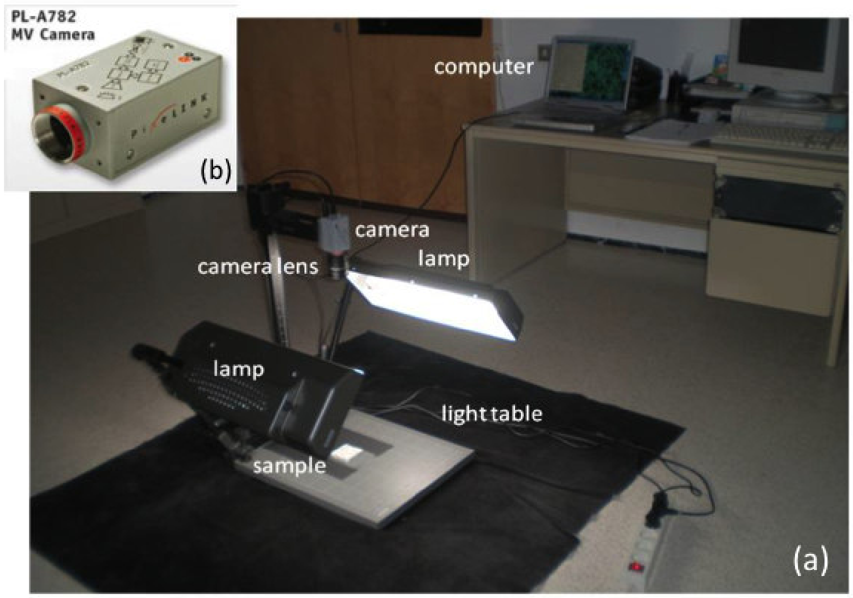

ACCEPTED MANUSCRIPT

ACCEPTED MANUSCRIPT

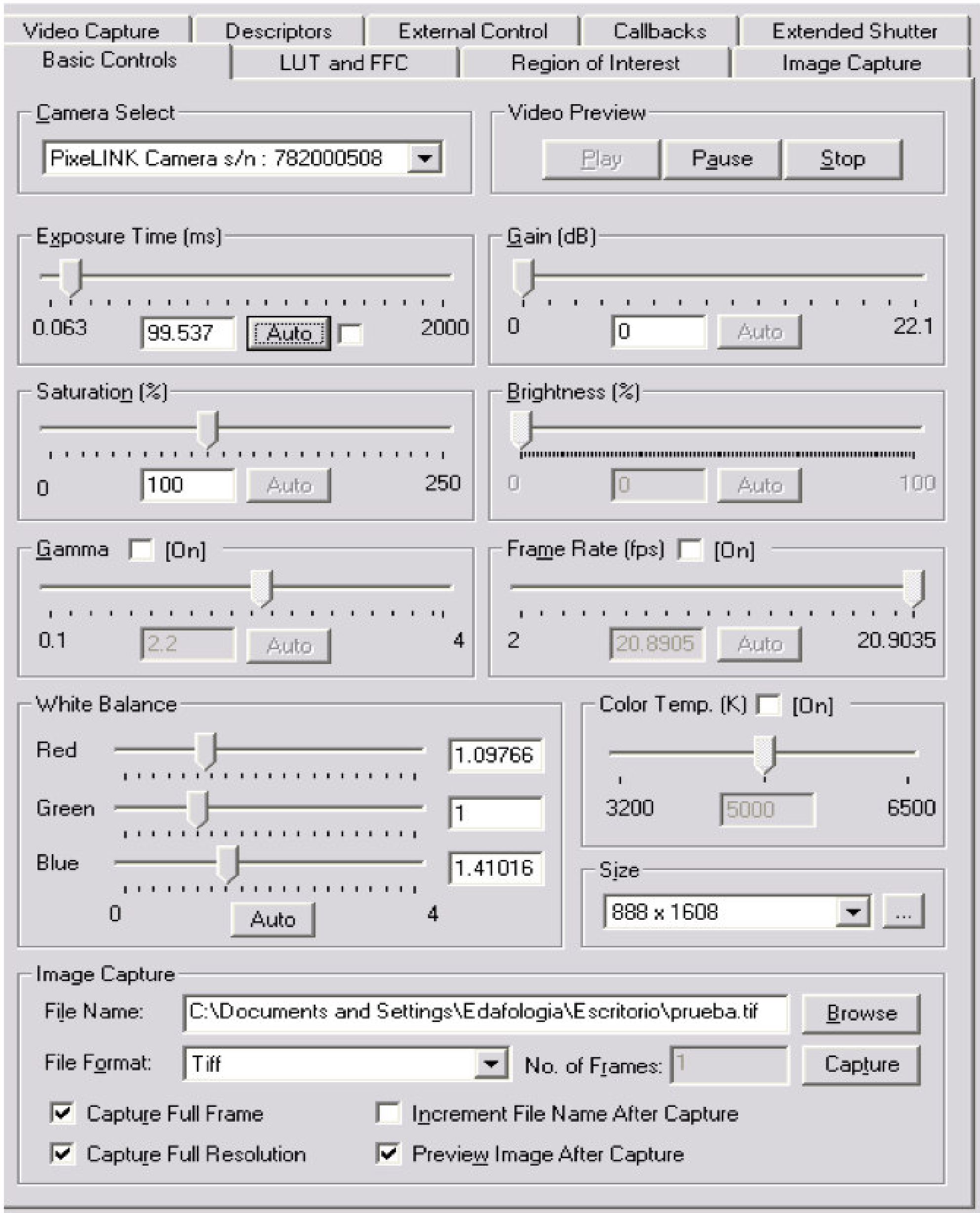

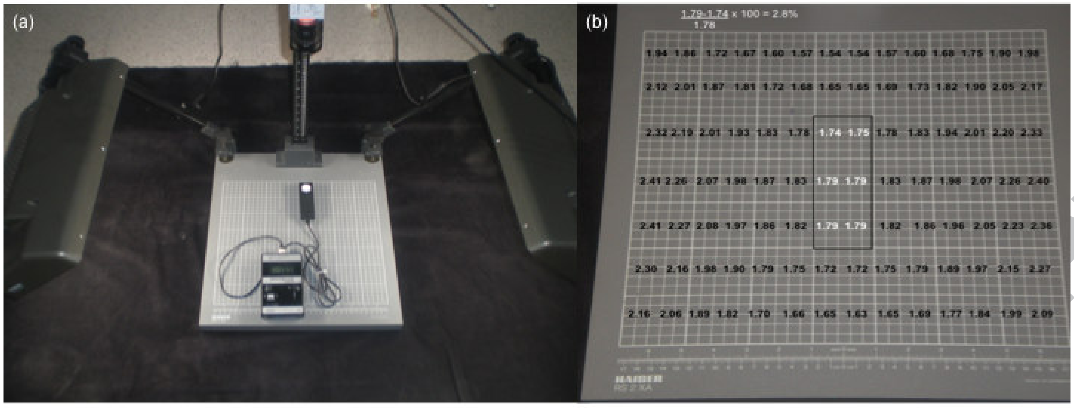

ACCEPTED MANUSCRIPT

ACCEPTED MANUSCRIPT

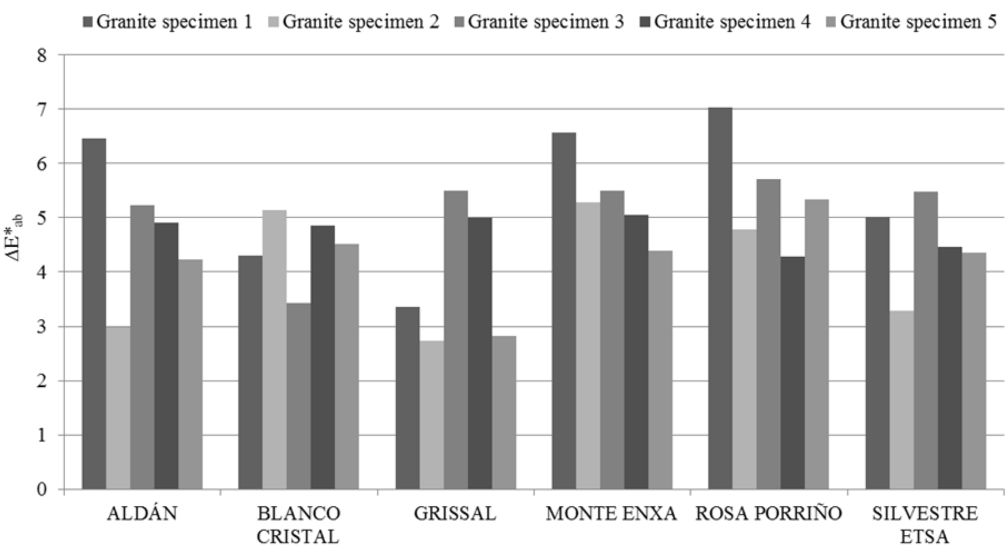

ACCEPTED MANUSCRIPT

ACCEPTED MANUSCRIPT

Table 1. Mineralogical and petrographic features of the types of granite under study.

Granite name	Location of Quarry	Macroscopic Aspect / Classification and Geochemistry	Textural Characteristics	Mineral Composition
Aldán	Area of Morrazo (Pontevedra, Spain)	Yellow-white, medium-, coarse-grained / Micaceous calcalkaline granite	Granoblastic heterogranular of coarse grain	Quartz (35%), Feldespar-K (21%), Plagioclases (23%), Biotite (10%), Moscovite (10%)
Blanco Cristal	Cadalso de los Vidrios pluton (Madrid, Spain)	White, medium-grained / Biotite adamellitic granite	Heterogranular-panallatriomorphic of medium grain	Quartz (26%), Feldespar-K (29%), Plagioclases (27.5%), Biotite (9%), Moscovite (2%), Clorite (4.5%)
Grissal	Rivadavia pluton (Ourense, Spain)	Grey coarse-grained / Alkaline granite	Porphyritic-panallatriomorphic of coarse grain	Quartz (30.5%), Feldespar-K (34.5%), Plagioclases (17.5%), Biotite (0.6%), Moscovite (0.5%), Clorite (3.5%)
Monte Enxa	Area of Barbanza (A Coruña, Spain)	White, medium-, coarse-grained / Two mica granite	Heterogranular-allatriomorphic of medium-, coarse-grain	Quartz (45%), Feldespar-K (18%), Plagioclases (12%), Biotite (7%), Moscovite (17%)
Rosa Porriño	Porriño pluton (Pontevedra, Spain)	Pinkish, coarse-grained granite / Biotite adamellitic	Porphyritic-panallatriomorphic of coarse grain	Quartz (30%), Feldespar-K (33%),

ACCEPTED MANUSCRIPT

ACCEPTED MANUSCRIPT

		granite		Plagioclases (21%), Biotite (9%), Clorite (3.5%)
Silvestre	Area of Vigo (Pontevedra, Spain)	White medium-grained with some ochre spots due to biotite weathering / Two mica adamellitic granite	Equigranular-panallatriomorphic of medium grain	Quartz (29%), Feldespar-K (26%), Plagioclases (24%), Biotite (8%), Moscovite (8%), Clorite (3.5%)

Petrographic characteristics and mineral composition described in [31, 55, 56].

ACCEPTED MANUSCRIPT

ACCEPTED MANUSCRIPT

Table 2. Average, maximum and minimum total color differences between the measured and the estimated CIELAB color stimuli, of the 212 color patches from the glossy and matte Munsell collection.

		SCI		SCE	
		8-bits	**10-bits**	**8-bits**	**10-bits**
ΔE^*_{ab}	Average	2.0	**1.9**	1.5	1.7
	Maximum	8.7	**6.9**	9.9	10.5
	Minimum	0.1	**0.2**	0.2	0.1
ΔE_{94} (2:1:1)	Average	1.2	**1.2**	1.1	1.2
	Maximum	4.4	**3.9**	5.0	5.4
	Minimum	0.1	**0.1**	0.2	0.1
ΔE_{94} (1:1:1)	Average	1.8	**1.8**	1.4	1.5
	Maximum	8.7	**6.9**	9.9	10.5
	Minimum	0.1	**0.2**	0.2	0.1
ΔE_{00} (2:1:1)	Average	**1.7**	1.7	1.4	1.5
	Maximum	**3.8**	4.1	4.5	4.6
	Minimum	**0.1**	0.1	0.1	0.1
ΔE_{00} (1:1:1)	Average	1.7	**1.7**	1.4	1.5
	Maximum	6.5	**5.8**	6.3	6.7
	Minimum	0.1	**0.2**	0.2	0.1
CMC (2:1)	Average	1.1	**1.1**	1.1	1.3
	Maximum	3.9	**3.7**	8.0	8.4
	Minimum	0.1	**0.1**	0.1	0.1
CMC (1:1)	Average	1.5	**1.5**	1.4	1.5
	Maximum	7.8	**6.3**	15.8	16.4
	Minimum	0.1	**0.2**	0.2	0.1

In order to select the optimal camera conditions, the lowest maximal value of the total color differences was used as a selection criterion. The optimal camera conditions, according to this criterion, for 8- and 10-bit data, are highlighted in bold in the table for each color difference formulae calculated using SCI or SCE data.

ACCEPTED MANUSCRIPT

ACCEPTED MANUSCRIPT

Table 3. Absolute and relative discrepancies between the spectrophotometer and the digital camera in the measurement of ΔE^*_{ab} total color difference.

	Absolute Discrepancy D_i	Relative Discrepancy D^r_i
Average ± SD	1.32 ± 1.06	0.06 ± 0.08
Maximum	6.41	0.84
Minimum	0.00	0.00

ACCEPTED MANUSCRIPT

ACCEPTED MANUSCRIPT

Table 4. Summary table of precision and tolerance (in CIELAB units) of the instrumental devices used.

	nΔE^*_{ab} (Precision)	Instrumental tolerance
Spectrophotometer	0.01	0.1
Digital camera	0.24	2.4

ACCEPTED MANUSCRIPT

ACCEPTED MANUSCRIPT

Highlights:

- We develop the fine-tuning of a method for the remote color measurement of granite.
- It is reported the description of a affordable methodology with digital camera.
- We estimate the effect of uncertainty on the measurement result.
- Choice combination of camera and spectrophotomer minimizes uncertainty of measurement.
- The calibrated camera was successfully used on granite stones.

ACCEPTED MANUSCRIPT